

Receiver extension method for a robust FWI

Towards a time-dependent relocalization

Student: M. Benziane

Supervisors: L. Métivier and R. Brossier

Friday 17th June, 2022



1. Introduction
2. Receiver extension strategy review (Métivier and Brossier, 2022)
3. Introducing a time dependence
4. Numerical application
5. Conclusion

Introduction

Introduction: FWI briefly

- FWI is a high resolution seismic imaging technique
- Ideally, all the phases in a waveform are considered
- FWI is formulated as a PDE constrained optimization, and is solved using local optimization

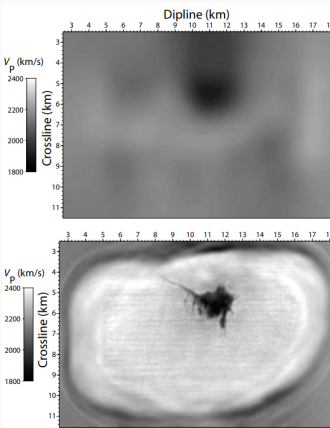


Figure 1: Depth slices from the Valhall field reconstructed velocity models (figure obtained from Virieux and Operto (2009) courtesy to L. Sirgue and O. I. Barkved, BP)

- FWI is a high resolution seismic imaging technique
- Ideally, all the phases in a waveform are considered
- FWI is formulated as a PDE constrained optimization, and is solved using local optimization

$$\min_m f(m) = \frac{1}{2} \sum_{s=1}^{N_s} \| \text{calculated} - \text{observed} \|^2 \quad (1)$$

Introduction: Cycle Skipping

- Cycle skipping occurs when $\Delta t > \frac{T}{2}$
- When using local optimization FWI may converge to a local minimum

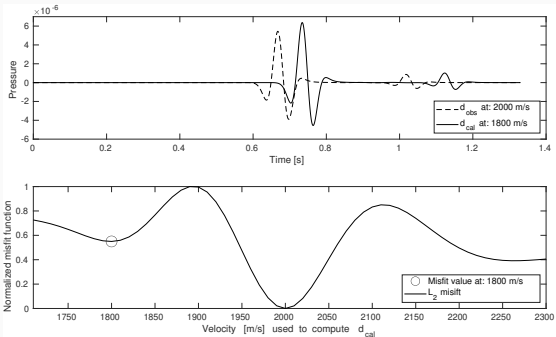


Figure 2: Simple numerical experiment to demonstrate the cycle skipping effect.

Introduction: Cycle skipping mitigation

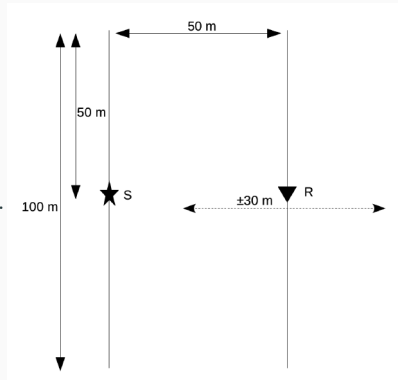
- Hierarchical schemes (Bunks et al., 1995)
- Alternative misfit functions (Van Leeuwen and Mulder, 2010; Métivier et al., 2016; Luo and Sava, 2011)
- Extension methods, such as model based extension methods (MVA) , source extension: MSWI, WRI (Symes, 2008) — (Huang et al., 2018a,b, 2019) — (van Leeuwen and Herrmann, 2013)

Receiver extension strategy review

(Métivier and Brossier, 2022)

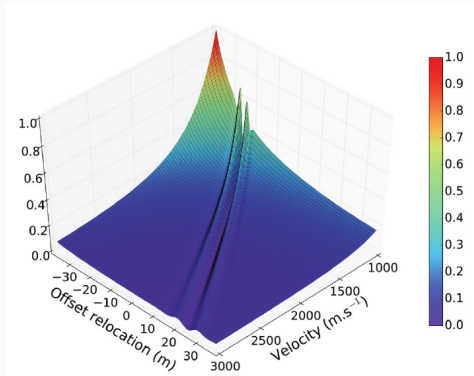
Receiver extension strategy

$$\min_{m, \Delta x} f(m, \Delta x) = \frac{1}{2} \sum_{s=1}^{N_s} \| \text{calculated_at_new_position} - \text{observed} \|^2 \dots \\ \dots + \alpha \text{ annihilator_on_receiver_position}$$

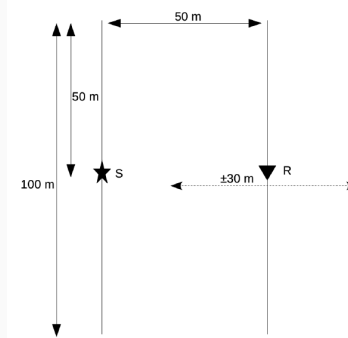


(Métivier and Brossier, 2022)

Receiver extension strategy: A transmission case



(a) Normalized misfit for the transmission case, α is taken as one



(b) Transmission numerical experiment

Figure 3: Transmission case analysis (Métivier and Brossier, 2022)

Receiver extension strategy: A transmission case

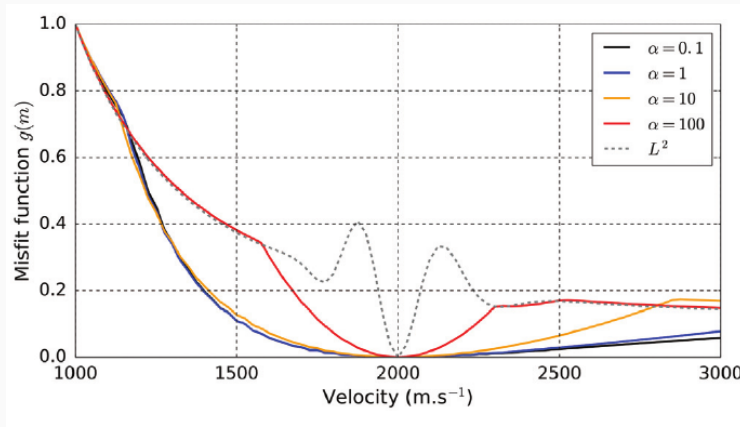


Figure 4: Normalized misfit for the transmission case (Métivier and Brossier, 2022)

Receiver extension strategy: Conclusion

- Métivier and Brossier (2022) promising results encourage the investigation of a time-dependent approach

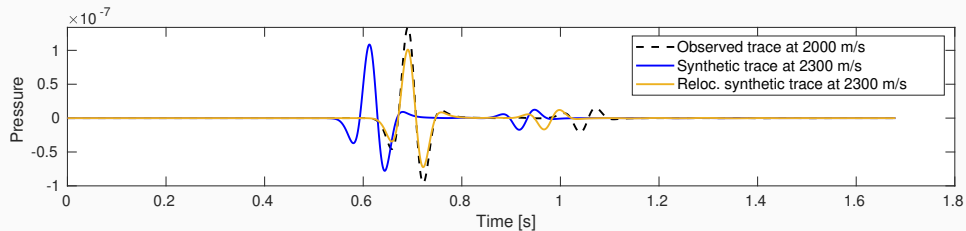


Figure 5: A simple two arrivals case, traces and receiver position correction, without time dependence

Introducing a time dependence

Introducing a time dependence

$$\min_{m, \Delta x} f(m, \Delta x) = \frac{1}{2} \sum_{s=1}^{N_s} \| \text{calculated_at_new_position}[t] - \text{observed} \|^2 + \dots \\ \dots \alpha \text{ annihilator_on_receiver_position}[t]$$

(2)

Introducing a time dependence: why?

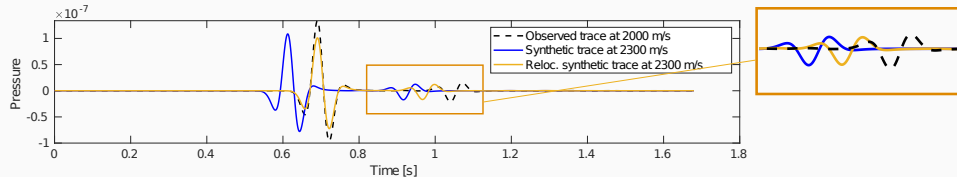


Figure 6: A simple two arrivals case, traces and receiver position correction, without time dependence

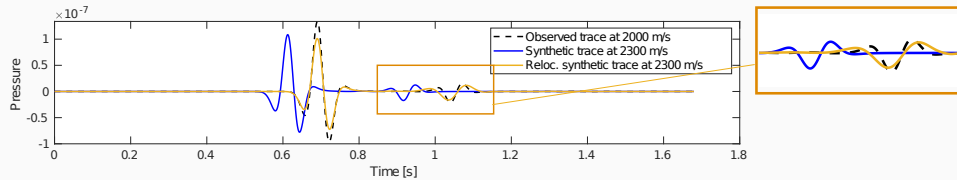


Figure 7: A simple two arrivals case, traces and receiver position correction, with time dependence

Introducing a time dependence

- The receiver can move with high speeds causing undesirable effects, a second annihilator is introduced

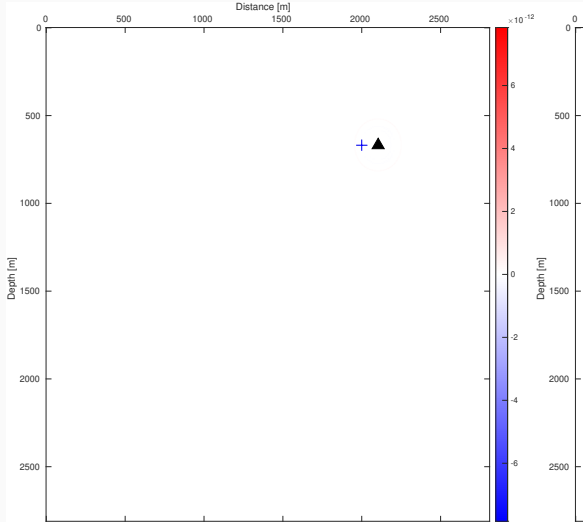
$$\min_{m, \Delta x} f(m, \Delta x) = \frac{1}{2} \sum_{s=1}^{N_s} \| \text{calculated at new position}[t] - \text{observed} \|^2 + \dots$$

(3)

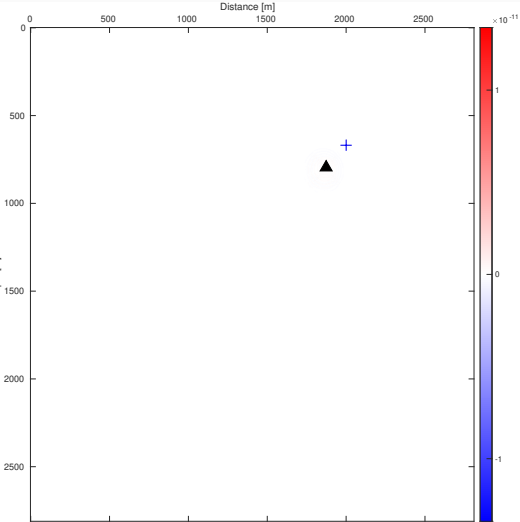
$$\dots \alpha \text{ annihilator_on_receiver_position}[t] + \beta \text{ annihilator_on_receiver_speed}[t]$$

Introducing a time dependence

With annihilator on receiver speed

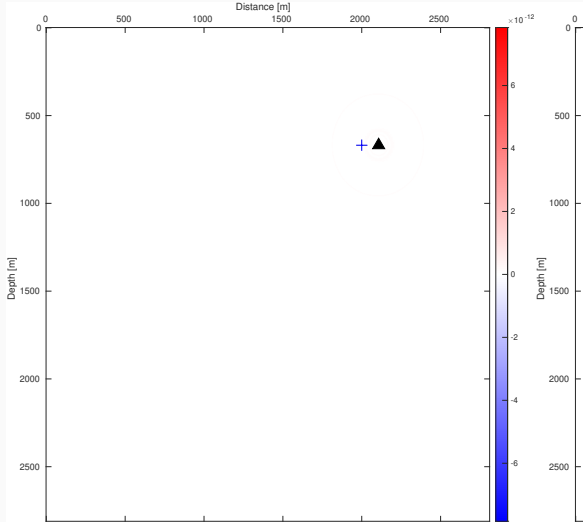


Without annihilator on receiver speed

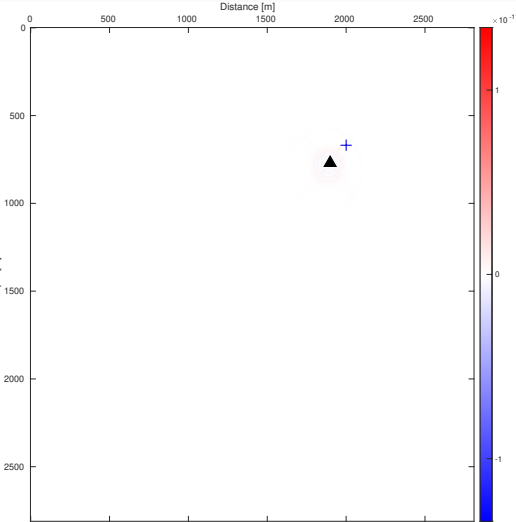


Introducing a time dependence

With annihilator on receiver speed

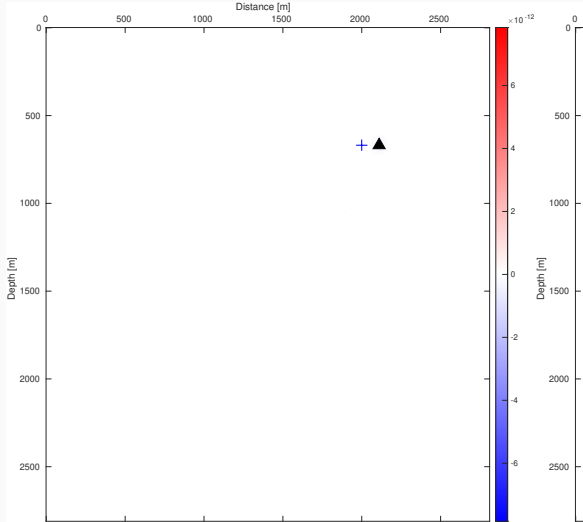


Without annihilator on receiver speed

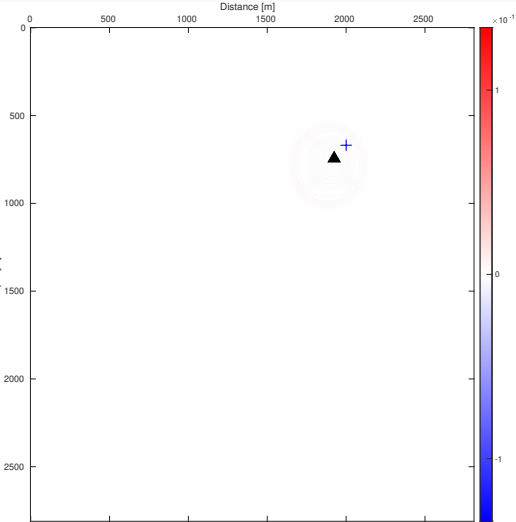


Introducing a time dependence

With annihilator on receiver speed

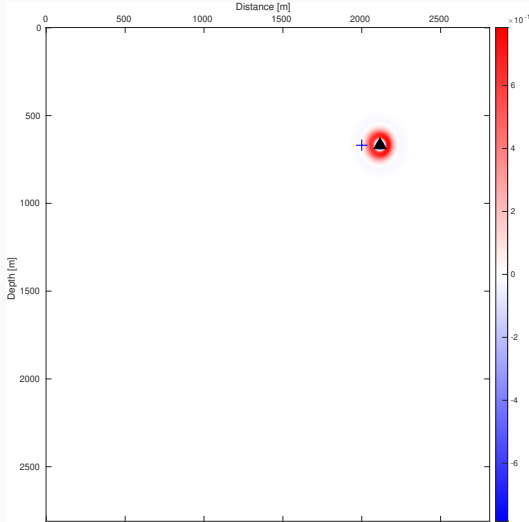


Without annihilator on receiver speed

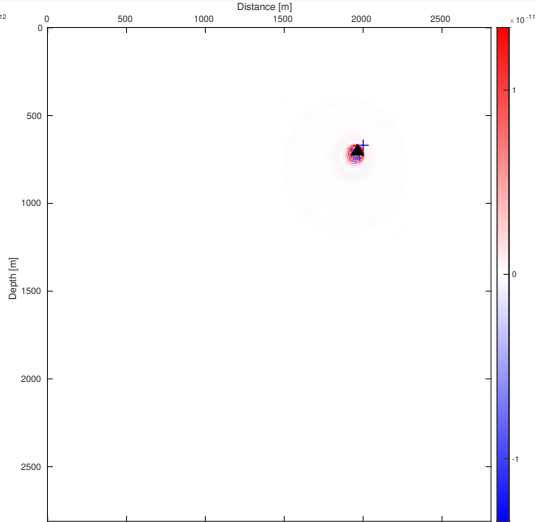


Introducing a time dependence

With annihilator on receiver speed

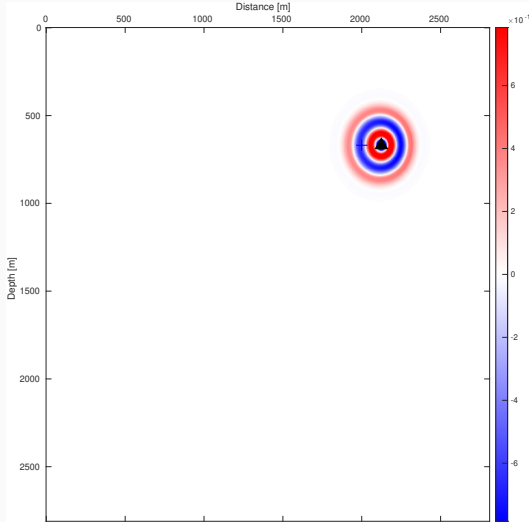


Without annihilator on receiver speed

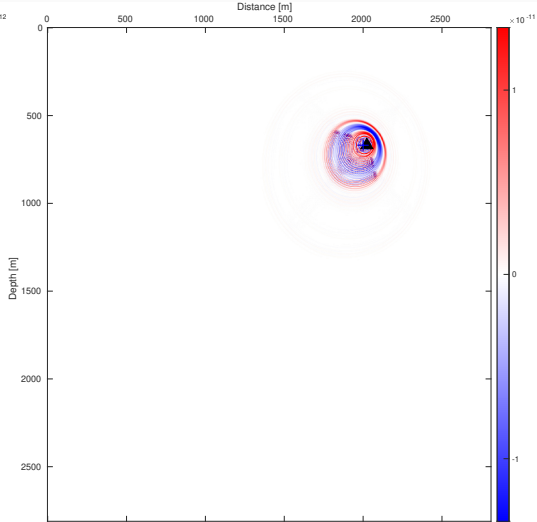


Introducing a time dependence

With annihilator on receiver speed

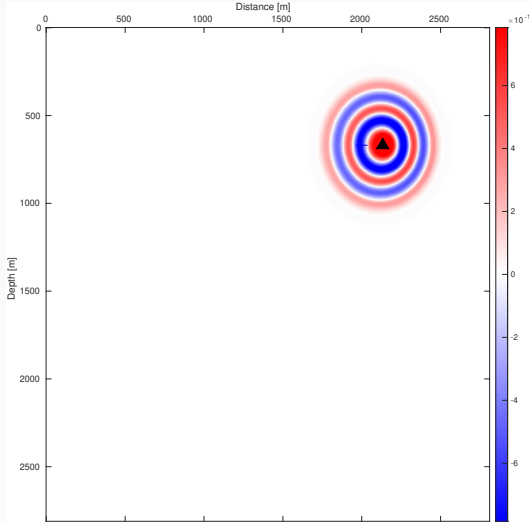


Without annihilator on receiver speed

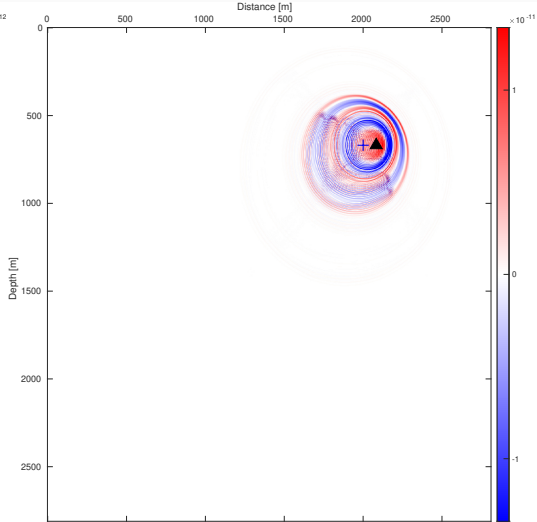


Introducing a time dependence

With annihilator on receiver speed

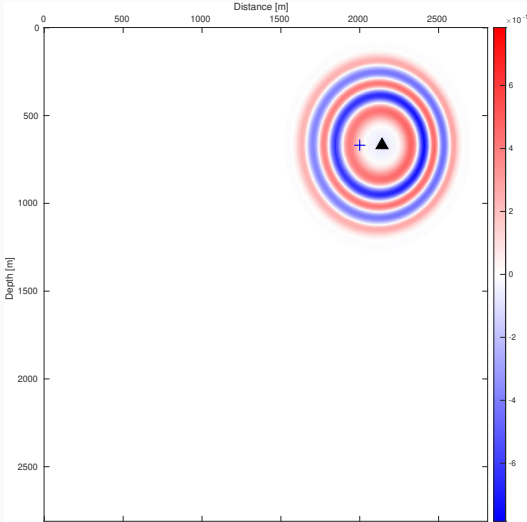


Without annihilator on receiver speed

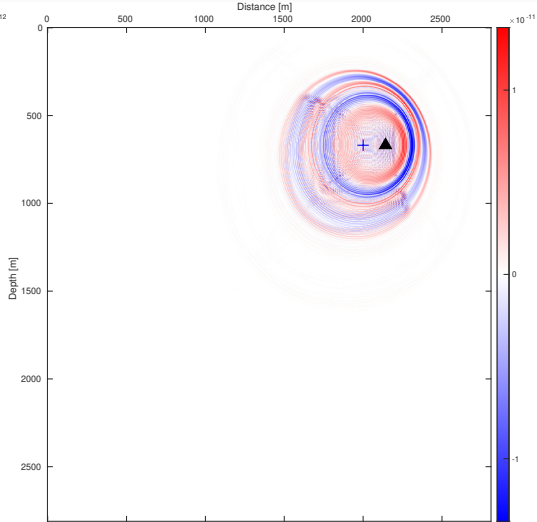


Introducing a time dependence

With annihilator on receiver speed

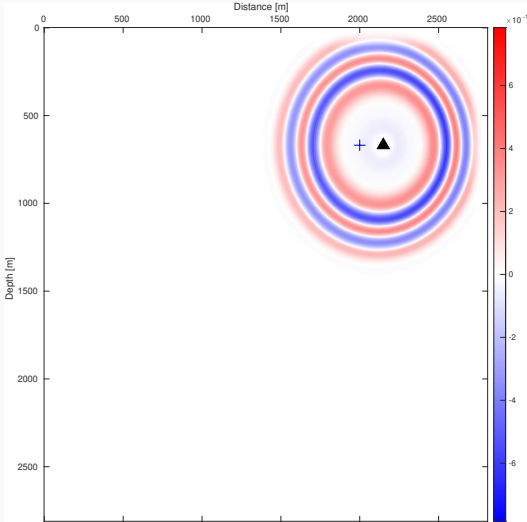


Without annihilator on receiver speed

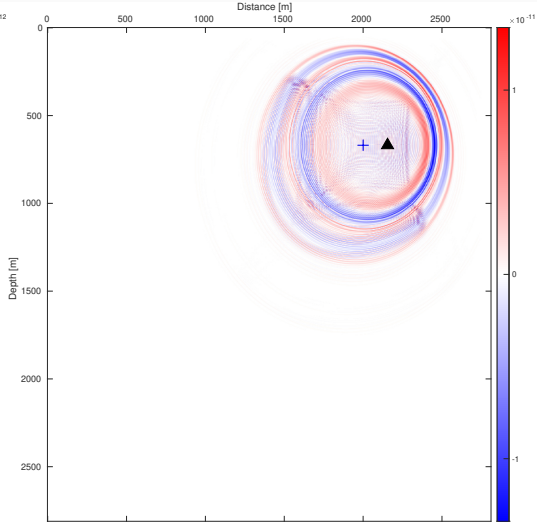


Introducing a time dependence

With annihilator on receiver speed

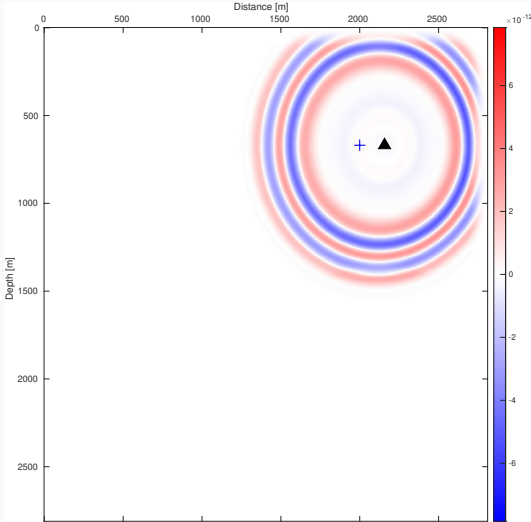


Without annihilator on receiver speed

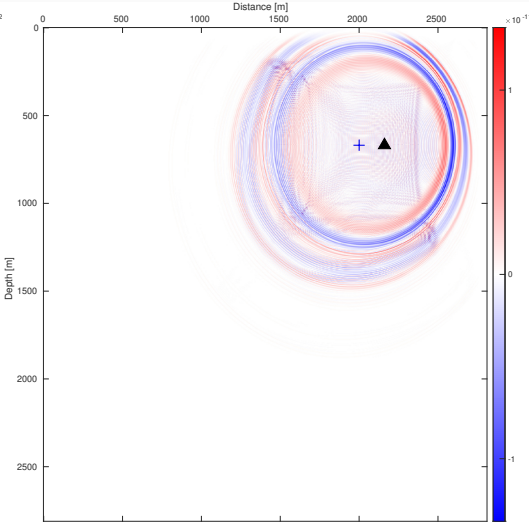


Introducing a time dependence

With annihilator on receiver speed

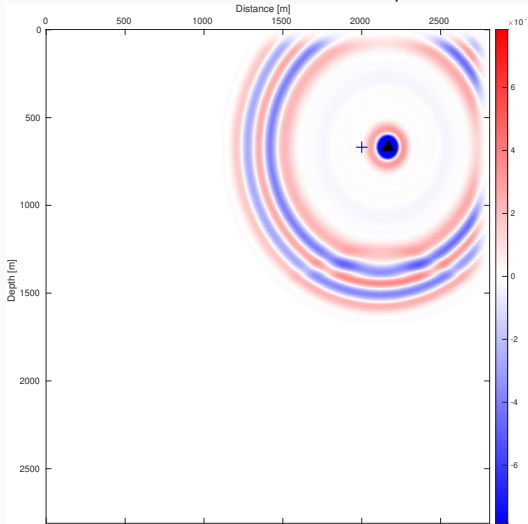


Without annihilator on receiver speed

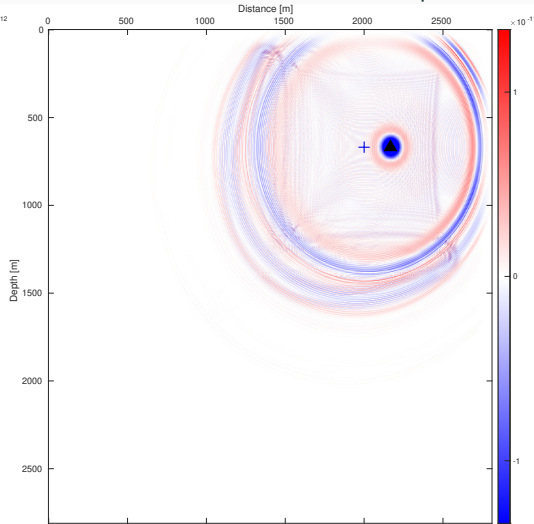


Introducing a time dependence

With annihilator on receiver speed

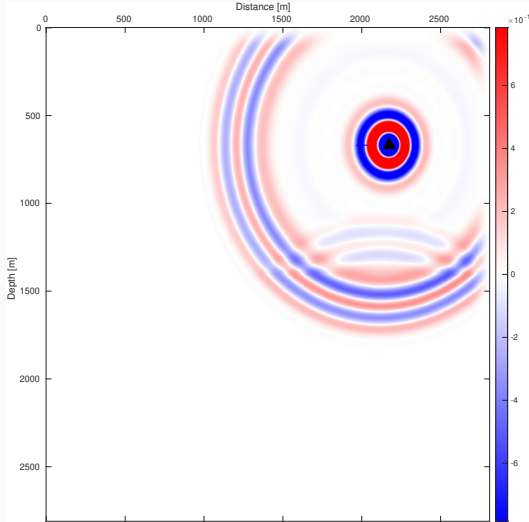


Without annihilator on receiver speed

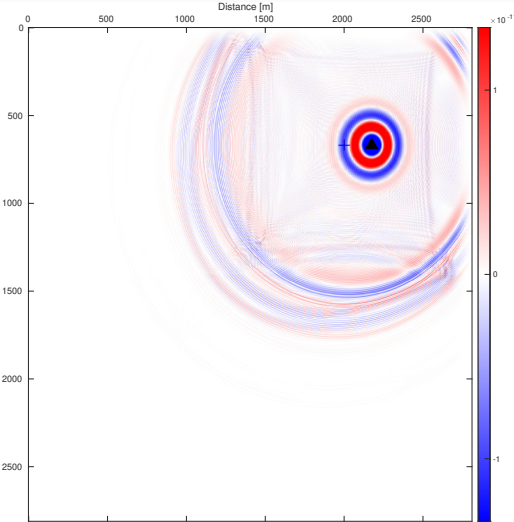


Introducing a time dependence

With annihilator on receiver speed

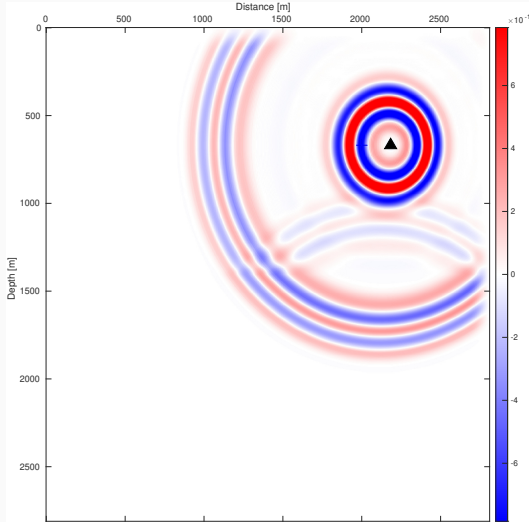


Without annihilator on receiver speed

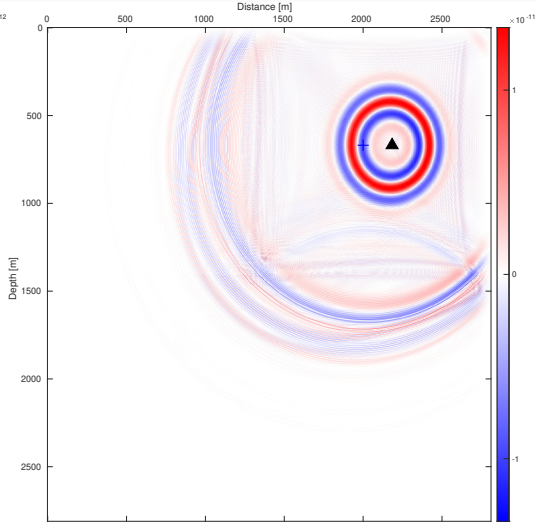


Introducing a time dependence

With annihilator on receiver speed

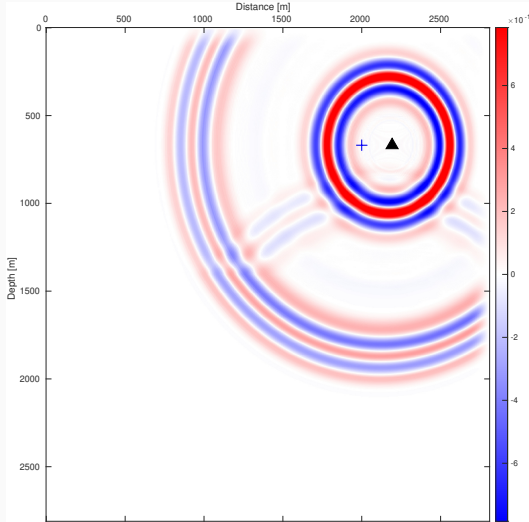


Without annihilator on receiver speed

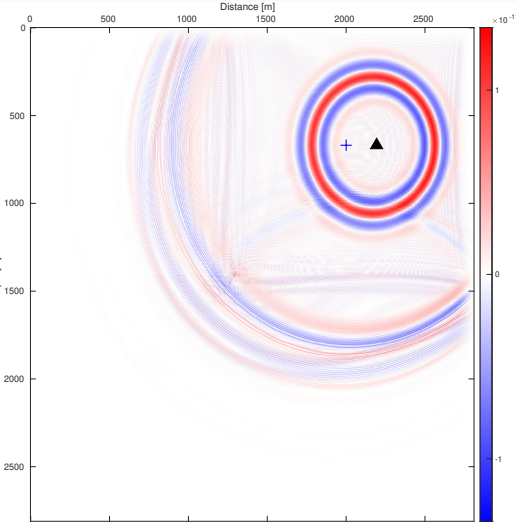


Introducing a time dependence

With annihilator on receiver speed

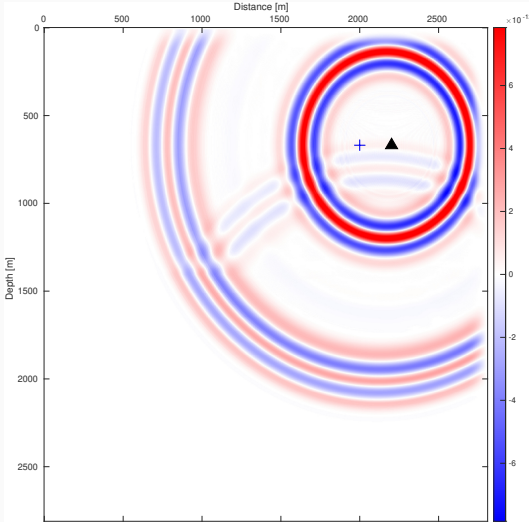


Without annihilator on receiver speed

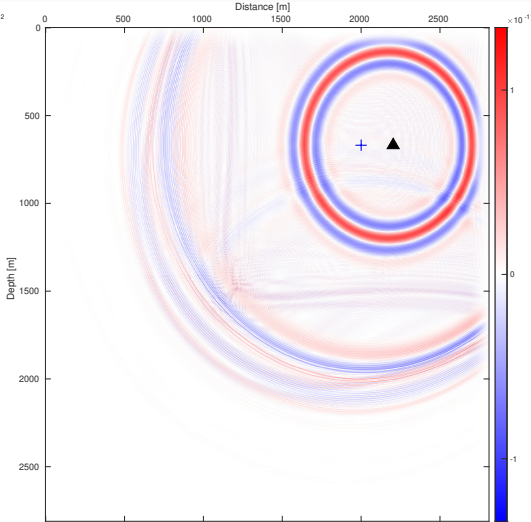


Introducing a time dependence

With annihilator on receiver speed

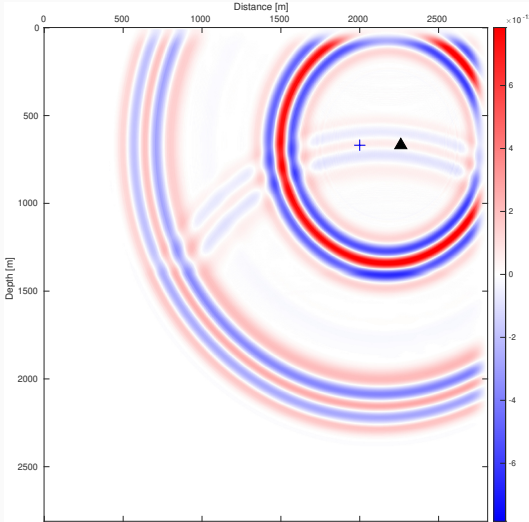


Without annihilator on receiver speed

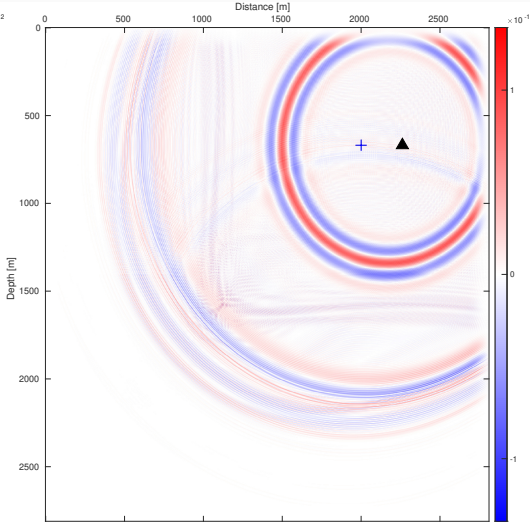


Introducing a time dependence

With annihilator on receiver speed

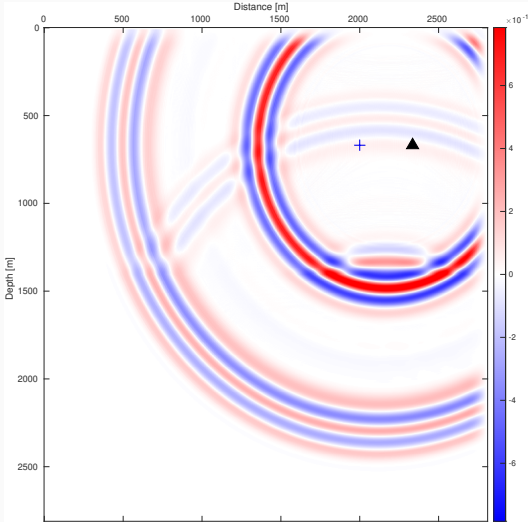


Without annihilator on receiver speed

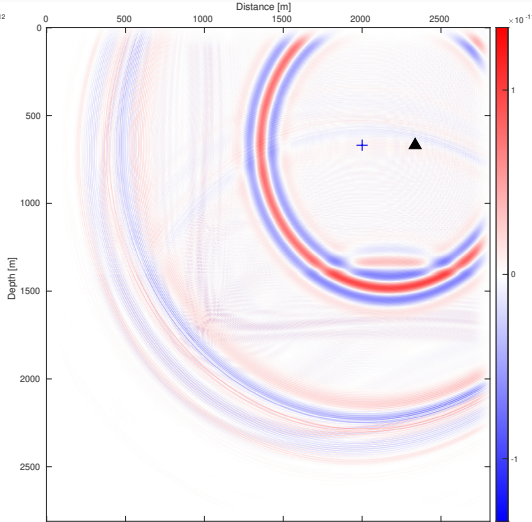


Introducing a time dependence

With annihilator on receiver speed

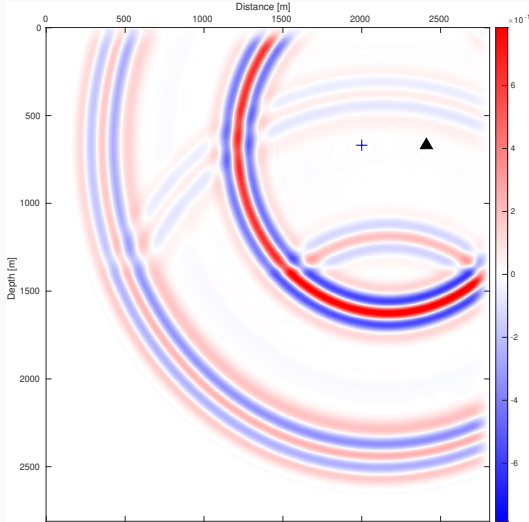


Without annihilator on receiver speed

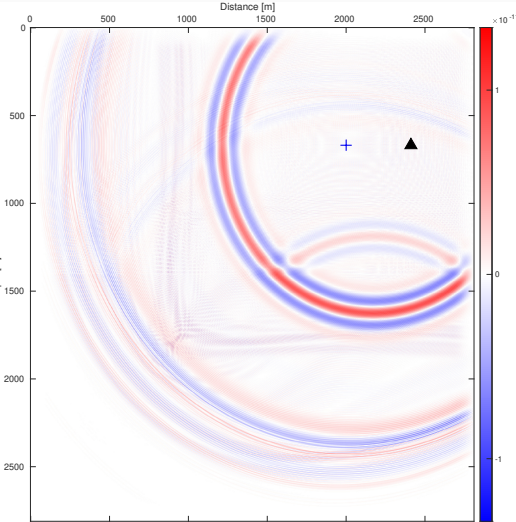


Introducing a time dependence

With annihilator on receiver speed

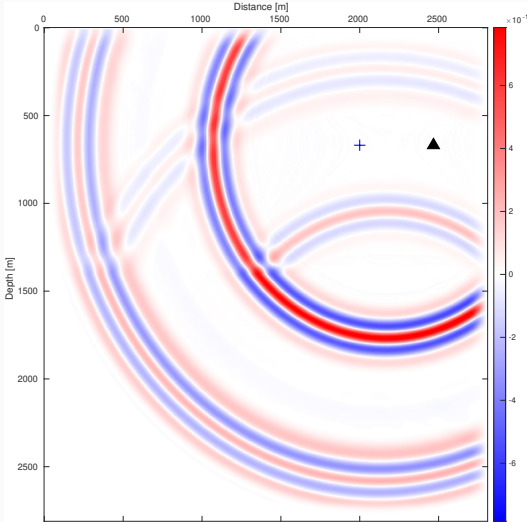


Without annihilator on receiver speed

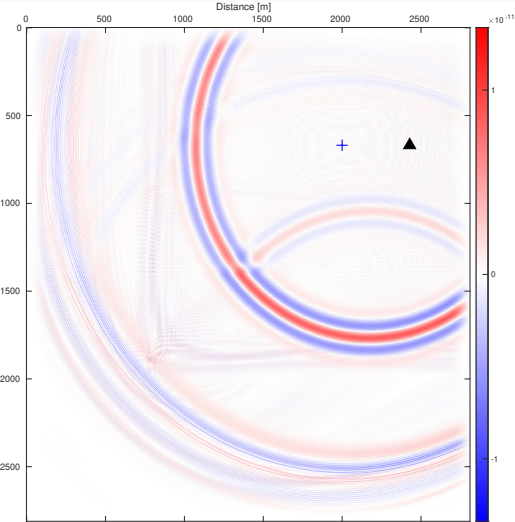


Introducing a time dependence

With annihilator on receiver speed

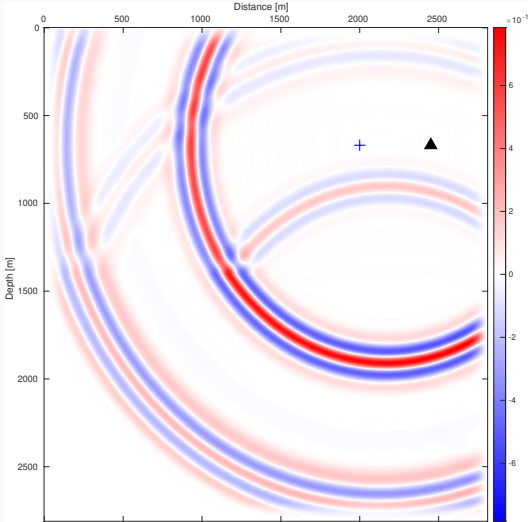


Without annihilator on receiver speed

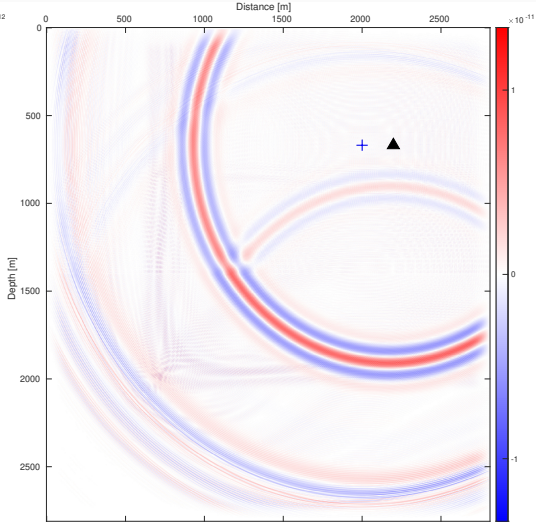


Introducing a time dependence

With annihilator on receiver speed

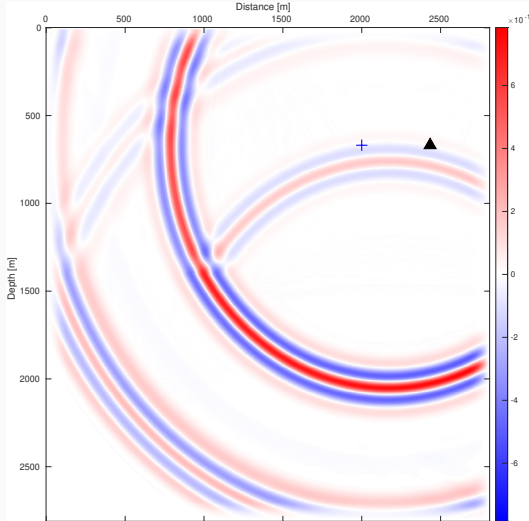


Without annihilator on receiver speed

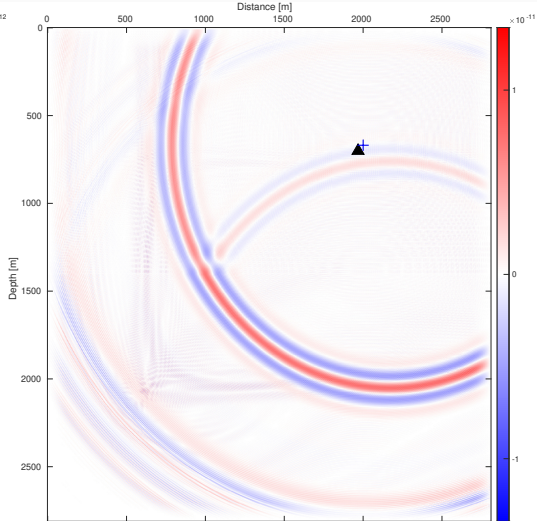


Introducing a time dependence

With annihilator on receiver speed

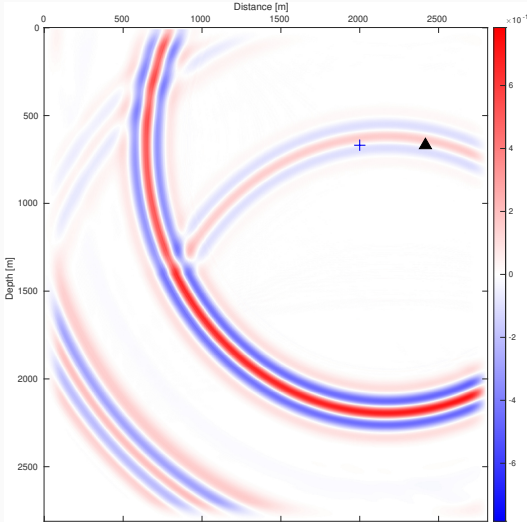


Without annihilator on receiver speed

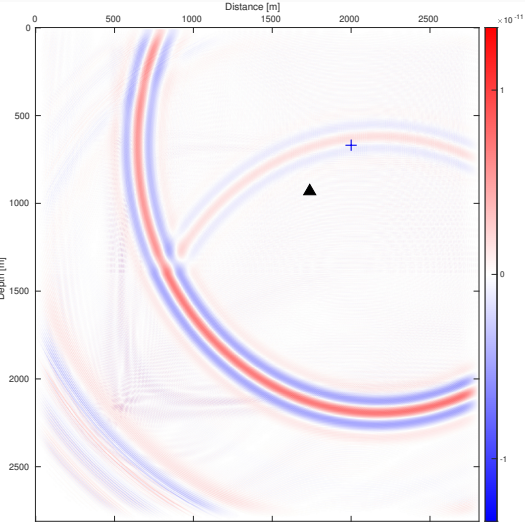


Introducing a time dependence

With annihilator on receiver speed



Without annihilator on receiver speed



Introducing a time dependence: Optimization methods

- MCMC implementations have been implemented and used for testing purposes
- We favor Very Fast Simulated Annealing -VFSA- (Ingber, 1993) thanks to the fast convergence
- VFSA converges in as little as 500 iterations (CPU time in the order of $\mathcal{O}(10^{-3})$ s)

Numerical application

Numerical application: Two layers case

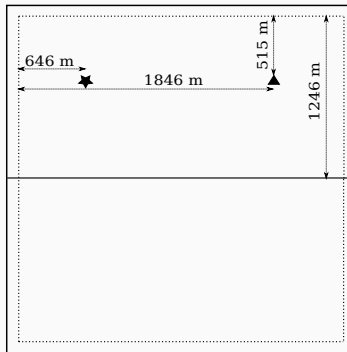


Figure 8: Simple two arrivals numerical experiment, the dashed line represent the start of the perfectly matched layer (PML).

Numerical application: two layers, high velocity case

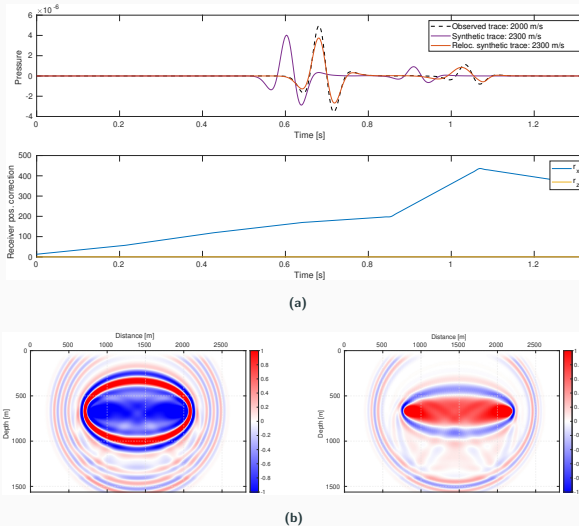


Figure 9: (a) Observed, calculated and relocated traces. (b) The corresponding sensitivity kernels. On the left panel we plot the sensitivity kernel without receiver relocation, on the right panel we compute the kernel at the extended receiver position.

Numerical application: two layers, low velocity case

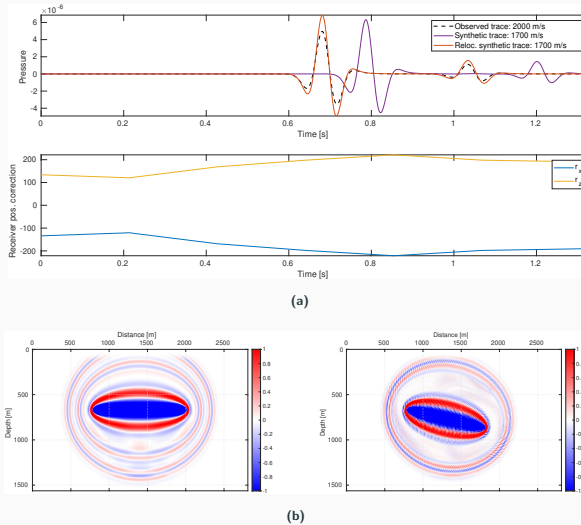


Figure 10: (a) Observed, calculated and relocated traces. (b) The corresponding sensitivity kernels. On the left panel we plot the sensitivity kernel without receiver relocation, on the right panel we compute the kernel at the extended receiver position.

Numerical application: two layers, misfit shape

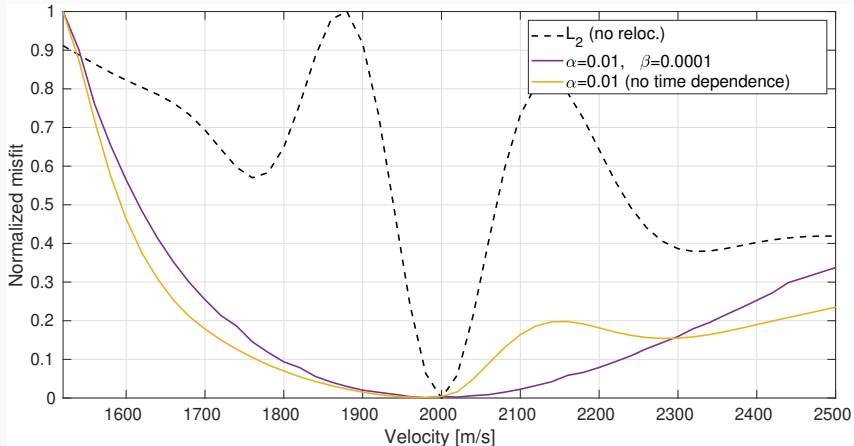


Figure 11: Misfit function variation versus the model velocity (homogeneous).

Numerical application: the Marmousi earth model

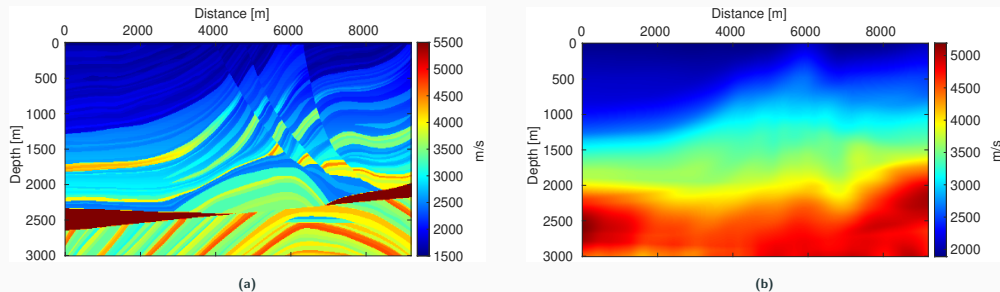


Figure 12: (a) The Marmousi earth model, (b) Gaussian smoothing and a 20% scaling are applied to the Marmousi model in Figure 12a.

Numerical application: the Marmousi earth model

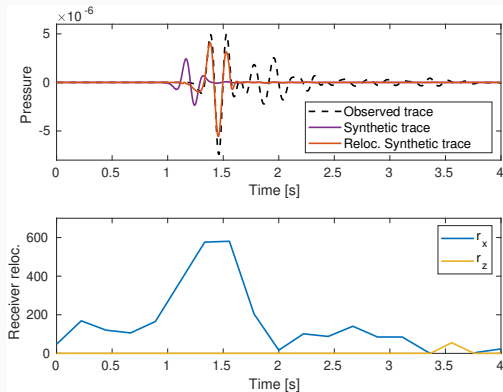
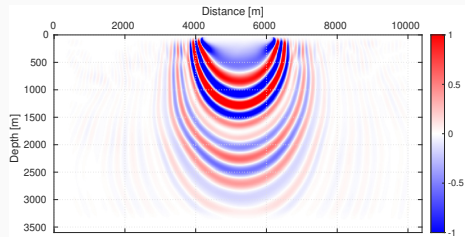
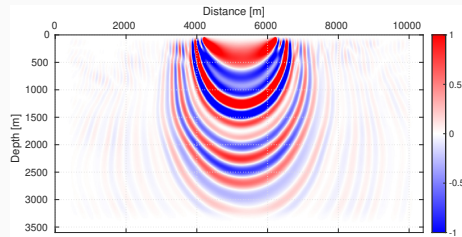


Figure 13: Observed and calculated traces with their corresponding relocalization profile, obtained from the smooth model in Figure 12b

Numerical application: the Marmousi earth model



(a) Standard FWI with cycle skipping



(b) FWI with receiver relocalization in time

Figure 14: Sensitivity kernels obtained in the Marmousi model shown in Figure 12b.

Conclusion

Conclusion:

- Encouraging results have been obtained at a reasonable cost using VFSA
- A second penalty term is added in order to constrain the receiver speed

Perspectives

- We will consider trans-dimensional optimization in order to have more flexibility on the parametrization
- Our optimization codes will be used in the next phase with the Seiscope package TOYxDAC, in order to carry out full FWI tests

Thank you for your attention and thanks to

- All my professors, notably, my supervisors
- CIMENT, Grenoble computing center
- All SEISCOPE project members

Questions?

References

- Bunks, C., Saleck, F. M., Zaleski, S., and Chavent, G. (1995). Multiscale seismic waveform inversion. *GEOPHYSICS*, 60(5):1457–1473.
- Huang, G., Nammour, R., and Symes, W. W. (2018a). Source-independent extended waveform inversion based on space-time source extension: Frequency-domain implementation. *GEOPHYSICS*, 83(5):R449–R461.
- Huang, G., Nammour, R., and Symes, W. W. (2018b). Volume source-based extended waveform inversion. *GEOPHYSICS*, 83(5):R369–R387.
- Huang, G., Nammour, R., Symes, W. W., and Dolliazal, M. (2019). *Waveform inversion via source extension*, pages 4761–4766.
- Ingber, L. (1993). Simulated annealing: Practice versus theory. *Mathematical and Computer Modelling*, 18(11):29–57.
- Luo, S. and Sava, P. (2011). *A deconvolution-based objective function for wave-equation inversion*, pages 2788–2792.
- Métivier, L. and Brossier, R. (2022). Receiver-extension strategy for time-domain full-waveform inversion using a relocalization approach. *GEOPHYSICS*, 87(1):R13–R33.
- Métivier, L., Brossier, R., Mérigot, Q., Oudet, E., and Virieux, J. (2016). Measuring the misfit between seismograms using an optimal transport distance: application to full waveform inversion. *Geophysical Journal International*, 205(1):345–377.
- Symes, W. W. (2008). Migration velocity analysis and waveform inversion. *Geophysical Prospecting*, 56(6):765–790.
- van Leeuwen, T. and Herrmann, F. J. (2013). Mitigating local minima in full-waveform inversion by expanding the search space. *Geophysical Journal International*, 195(1):661–667.
- Van Leeuwen, T. and Mulder, W. A. (2010). A correlation-based misfit criterion for wave-equation traveltime tomography. *Geophysical Journal International*, 182(3):1383–1394.
- Virieux, J. and Operto, S. (2009). An overview of full-waveform inversion in exploration geophysics. *Geophysics*, 74:WCC1–WCC26.

Introducing a time dependence: Analysis using ray theory

$$T_0^2 = \frac{x^2}{v_0^2} + \frac{4h^2}{v_0^2} \quad (4)$$

$$\bar{T}_1^2 = \frac{x^2}{v_1^2} + \frac{4h^2}{v_1^2} \quad (5)$$

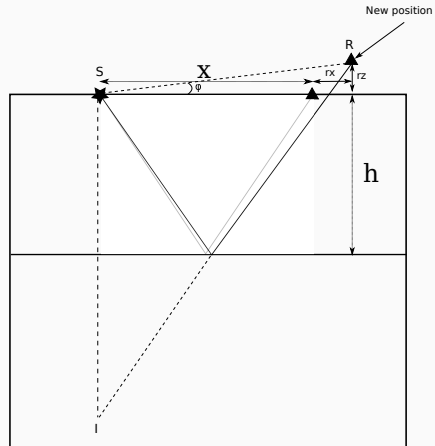
In order to obtain a fit ($T_1 = T_0$) in the wrong velocity model, the receiver position needs to be corrected. Introducing r_z and r_x

$$IR^2 = 4h^2 + SR^2 - 4hSR\cos(\phi + \frac{\pi}{2})$$

...

$$IR^2 = 4h^2 + (x + r_x)^2 + r_z^2 + 4hr_z \quad (6)$$

$$T_1^2 = \frac{1}{v_1^2} \left[r_z^2 + r_x^2 + 4hr_z + 2xr_x + x^2 + 4h^2 \right]$$

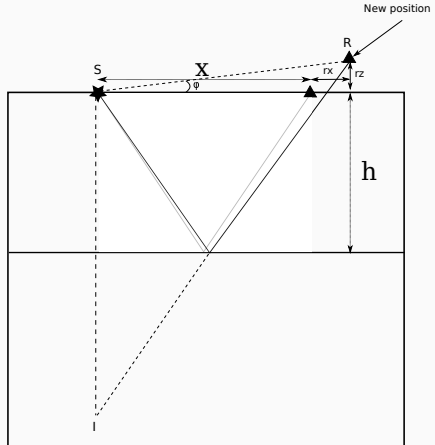


Introducing a time dependence: Analysis using ray theory

$$r_z^2 + r_x^2 + 4hr_z + 2xr_x + (4h^2 + x^2)\left(1 - \frac{v_1^2}{v_0^2}\right) = 0 \quad (7)$$

Equation 7 has the form the general form of a Cartesian conic section equation, a circle in this case, this can be simplified to a more standard form so we can retrieve the parameters

$$(r_z + 2h)^2 + (r_x + x)^2 = \left(4h^2 + x^2\right) \frac{v_1^2}{v_0^2} \quad (8)$$



Receiver extension strategy: Inner loop

- The inner problem is highly nonlinear, a global optimization scheme is employed¹
- The receivers corrections are allowed only to move horizontally

```
m1 ← m0;
while not(stop_criteria) do
    us ← ComputeForward (mk);
     $\Delta x_s \leftarrow \text{Gridsearch}(u_s, d_{obs})$ ; /* Inner loop
    */
    Risiduals ← R( $\Delta x_s(m_k)$ )us −  $d_{obs,s}$ ;
    λs ← ComputeAdjoint(Risiduals, us,  $\Delta x_s$ );
     $\nabla g(m_k) \leftarrow \text{ComputeGradient}(u_s, \lambda_s)$ ;
     $m_{k+1} \leftarrow m_k - \alpha_k Q(m_k) \nabla g(m_k)$ ;
    k ← k + 1
end
```

¹gridsearch at this stage

Receiver extension strategy: Outer loop

- The outer problem is solved using quasi-Newton strategy, and a preconditioned I-BFGS
- The calculated data as well as the gradient are computed using the corrected receivers positions

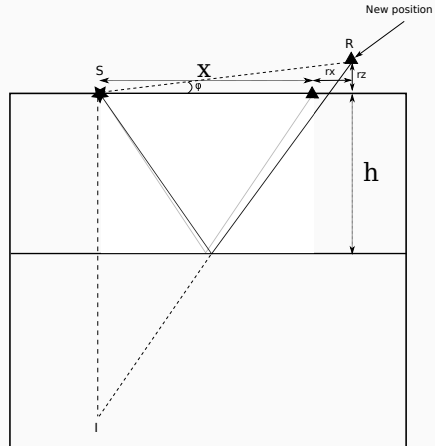
$$\nabla g(m) = \sum_{s=1}^{N_s} \left\langle \frac{\partial A}{\partial m} u_s, \lambda_s \right\rangle \quad (9)$$

$$\begin{cases} A(m)u_s = b_s \\ A(m)^T \lambda_s = R(\overline{\Delta x}_s(m))^T (R(\overline{\Delta x}_s(m))u_s - d_{obs,s}) \end{cases} \quad (10)$$

```
m1 ← m0;
while not(stop_criteria) do
    us ← ComputeForward (mk);
    Δxs ← Gridsearch(us, dobs) ; /* Inner loop */
    *
    Risiduals ← R(Δxs(mk))us − dobs,s;
    λs ← ComputeAdjoint(Risiduals, us, Δxs);
    ∇g(mk) ← ComputeGradient(us, λs);
    mk+1 ← mk − αk Q(mk)∇g(mk);
    k ← k + 1
end
```

Introducing th time dependence: Analysis using ray theory

- Allowing the receiver to move in the horizontal solution solely will not guarantee a fit for all arrivals in some cases (**next slides**)
- It is helpful to consider a simple case where the receiver is allowed to move in two directions



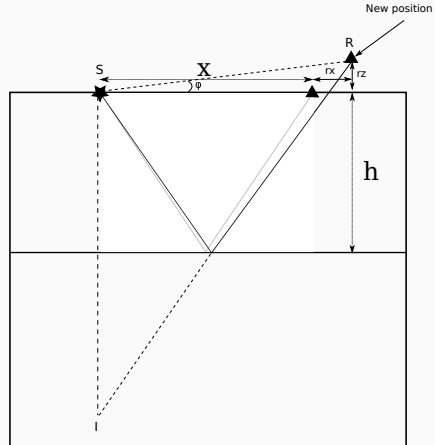
Introducing a time dependence: Analysis using ray theory

$$T_0^2 = \frac{x^2}{v_0^2} + \frac{4h^2}{v_0^2} \quad (11)$$

$$\bar{T}_1^2 = \frac{x^2}{v_1^2} + \frac{4h^2}{v_1^2} \quad (12)$$

In order to obtain a fit ($T_1 = T_0$) in the wrong velocity model, the receiver position needs to be corrected. Introducing r_z and r_x

$$(r_z + 2h)^2 + (r_x + x)^2 = (4h^2 + x^2) \frac{v_1^2}{v_0^2} \quad (13)$$



Introducing a time dependence: Analysis using ray theory

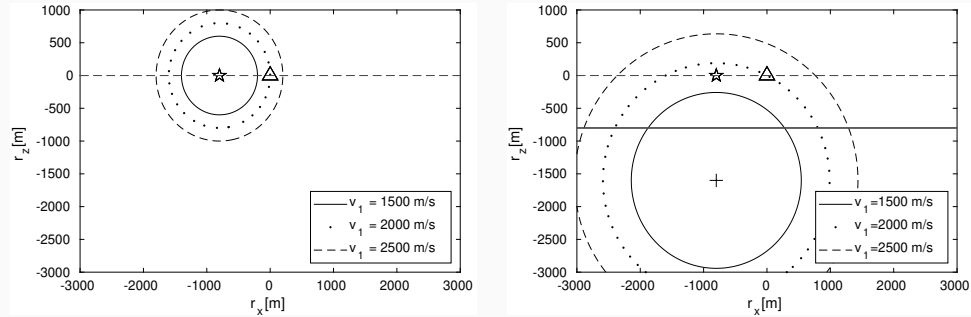
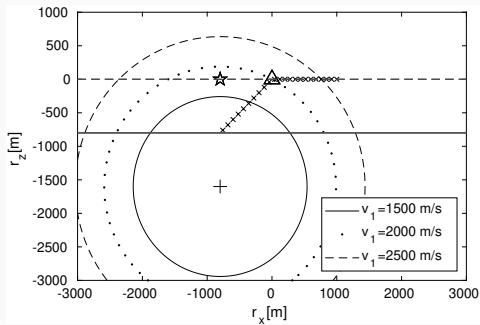


Figure 15: Variable velocity ratio — (Left): Direct arrival¹, (Right): Reflected arrival

¹Ray theory was used to obtain the transmitted isochrones, the analysis is not shown here

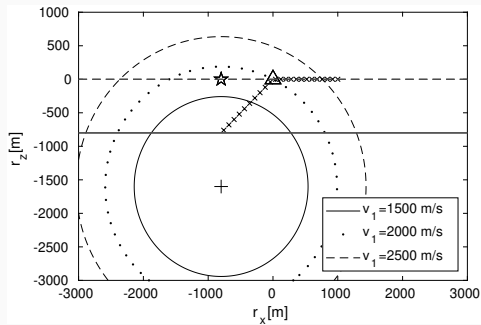
Introducing a time dependence: Analysis using ray theory

$$\begin{cases} r_z = |r_x|, & \text{If the receiver is to be moved toward the source} \\ r_z = 0, & \text{otherwise} \end{cases}$$



Introducing a time dependence: Analysis using ray theory

$$\begin{cases} r_z = |r_x|, & \text{if } \operatorname{sgn}(x_s - x_r)r_x > 0 \\ r_z = 0, & \text{otherwise} \end{cases} \quad (14)$$



Backup slide: penalty terms

$$\mathcal{P}_1 = \alpha \frac{\|d_{obs}\|_\infty}{2L} \|r(t)\|_2^2 \quad (15)$$

The relocalization can be written as $r(t) = \sqrt{r_x(t)^2 + r_z(t)^2}$. We write the L2 norm

$$\begin{aligned} \|r(t)\|_2 &= \left\{ \frac{1}{T} \int_0^T |r(t)|^2 dt \right\}^{\frac{1}{2}} \\ \|r(t)\|_2^2 &= \frac{1}{T} \int_0^T [r_x(t)^2 + r_z(t)^2] dt \end{aligned} \quad (16)$$

The integral can be evaluated as sum (equation 17) using Gauss-Legendre quadrature rule.

$$\int_0^T r_x(t)^2 dt \approx \sum_{i=1}^n w_i r_x(t_i)^2 \quad (17)$$

In the current implementation, a composite integral is used, whereby, the quadrature is computed in each element and summed for the entire domain.

Backup slide: penalty terms

In order to compute the norm of the velocity of the receiver, we compute the first time derivative of the relocalization components. First, we need to write the penalty term:

$$\mathcal{P}_2 = \frac{\beta}{2T} \frac{\|d_{obs}\|_\infty}{V_{max}} \int_0^T |V_r(t)|^2 dt \quad (18)$$

β is a tuning parameter. The receiver velocity can be written as follow

$$V_r(t) = \frac{dr(t)}{dt} = \frac{d}{dt} \sqrt{r_x(t)^2 + r_z(t)^2}$$
$$V_r(t) = \frac{r_x(t) \frac{dr_x}{dt} + r_z(t) \frac{dr_z}{dt}}{r(t)} \quad (19)$$

$$\frac{dr_x(t)}{dt} = \sum_{j=1}^{N+1} a_j \ell'_j(t), \quad \ell'_i(t) = \ell_i(t) \sum_{j=1, j \neq i}^{N+1} \frac{1}{t - t_j} \quad (20)$$